SMALL NONCODING RNA CONTENTS OF RAT EPIDIDYMAL EXTRACELLULAR VESICLES INCLUDING A PUTATIVE NOVEL SMALL RNA

Running Head: Small noncoding RNAs in epididymal EVs

Keywords: sncRNA, extracellular vesicles, epididymis, epididymosomes, miRNA, tRNA fragments, CpG islands, rat

Ross Gillette[1], Shyamal Waghwala[2], Andrea C. Gore[1†]

[1] The Center for Molecular Carcinogenesis and Toxicology, Division of Pharmacology and Toxicology, College of Pharmacy, The University of Texas at Austin, Austin, TX, 78712, USA

[2] College of Natural Sciences, The University of Texas at Austin, Austin, TX, 78712, USA

AUTHOR CONTRIBUTIONS

Conceptualization: R.G.; Methodology: R.G.; Investigation: R.G.; Formal Analysis: R.G., S.W.; Writing – Original Draft: R.G.; Writing – Review & Editing: R.G., A.C.G.; Funding Acquisition: R.G., A.C.G.

[†] Corresponding Author: andrea.gore@austin.utexas.edu

ABSTRACT

Extracellular vesicles (EVs) released from the epididymal epithelium (epididymosomes) impart functional competence on sperm as they transit the epididymis by merging with sperm and releasing a complex repertoire of molecules. The cargo of epididymosomes includes small noncoding RNAs (sncRNAs) that are modified by external factors such as stress, nutrition, and drug use. If incorporated into sperm, the EV sncRNA cargo can affect offspring and lead to heritable phenotypes. In the current study we characterized the RNA contents of EVs collected from the caput epididymis of adult male rats in order to fill a gap in knowledge in this species and to establish a sncRNA profile. Small RNAs of EVs were isolated from the caput portion of the epididymis of adult male rats, and sequenced on a NovaSeq 6000 on a SP flow cell in a single-end 50 bp configuration. The resulting reads were checked for quality, trimmed for adapter sequences, aligned to the unmasked rat genome (Rnor 6), and assigned an annotation designation. The majority of RNA reads aligned to either tRNA fragments (79.1%) or piRNA (18.1%) loci. Micro RNAs (miRNAs) accounted for a surprisingly small proportion of reads (0.18%). The third largest category of aligned reads (1.5%) was in intergenic space and not strictly associated with canonical sncRNA loci. In-depth investigation determined these latter reads (~19 nt) aligned strictly within the boundaries of known CpG islands (CpGi), which have not previously been reported to express any form of sncRNA. These newly described "CpGi sRNAs" could not consistently be accounted for by overlaying features of any other annotation type (including rRNA and piRNA). The CpGi sRNAs have characteristics of RNA fragments that can associate with the Argonaute/PIWI family of proteins and therefore could have regulatory function via RNA induced silencing or de novo DNA methylation. We propose that CpGi sRNAs constitute a new family of sncRNA that may represent an important and unreported class of regulatory RNA in gametes.

24 **INTRODUCTION**

25 Spermatozoa are incapable of fertilization as they exist the testes [1] and only gain motility
26 and the capacity for fertilization as they transit the epididymis [2]. This process requires
27 epididymosomes [3–6], a type of extracellular vesicle (EV) within the microvesicle category [7–
28 9]. Epididymosomes are released from the epididymal epithelium via apocrine secretion [10], fuse
29 to spermatozoa [11], aid in their maturation and functionalization [4,12,13], and mark dead or
30 dying spermatozoa for elimination [14,15]. Epididymosomes carry a complex repertoire of ions,
31 proteins and small non-coding RNAs (sncRNA) [4,12,16,17] that are transferred to [18,19] and
32 presumably alter the function of the spermatozoa or impart functional consequences on the
33 fertilized embryo [20]. Importantly, sncRNA molecules transferred to spermatozoa have the
34 capacity to alter the epigenetic landscape of either the spermatozoa or the fertilized embryo and
35 thereby influence subsequent generations. Furthermore, the sncRNA contents of epididymosomes
36 are subject to modification by the hormonal milieu [21,22] and environmental challenges such as
37 psychosocial or metabolic stress [22–27], making them a potential vector for intergenerational
38 effects in offspring. This key role was illuminated by studies showing that early life stress caused
39 behavioral and physiological changes in the offspring, phenotypes that were recapitulated by
40 microinjection of a small number of microRNAs into a fertilized egg subsequently used for *in vitro*
41 fertilization [28,29].

42 The sncRNA repertoire of epididymosomes is complex and diverse [30]. The most
43 abundant sncRNA found in epididymosomes is microRNA (miRNA) followed by smaller
44 proportions of transfer RNA (tRNA) and ribosomal RNA (rRNA) [25,30,31]. The remainder
45 consists of piwi-interacting RNA (piRNA), small nuclear RNA (snRNA), and small nucleolar
46 RNA (snoRNA), as well as long non-coding RNA (lncRNA) [25]. Other species of sncRNA, such
47 as YRNA and Vault RNA, have not yet been reported in epididymosomes but should not be ruled
48 out for inclusion in these complex profiles. Furthermore, there are likely additional sncRNAs yet
49 to be identified [32].

50 Much of the knowledge we have on the sncRNA contents of caput epididymosomes, which
51 are crucial for the final steps of spermatozoa maturation, is from mouse models. Very little has
52 been reported on the epididymosomes of rats, which are an important model system for
53 endocrinology, reproduction, and epigenetic transgenerational inheritance, and in which
54 behavioral work is considered to better translate to humans [33–35]. Here, we characterized the
55 contents of EVs derived from the caput epididymis of the male rat and describe what we believe
56 to be a previously undefined class of sncRNA.

57

58 **MATERIALS AND METHODS**

59 **Animals and treatment**

60 All animal experiments were conducted using humane procedures that were pre-approved
61 by the Institutional Animal Care and Use Committee at The University of Texas at Austin and in
62 Accordance with NIH guidelines. Three-month old male and female Sprague Dawley rats were
63 purchased (Envigo, Indianapolis, IN) and shipped to the Animal Resource Center at the University
64 of Texas at Austin and allowed two weeks to acclimate to the housing facility. All animals in the
65 colony were housed in a room with consistent temperature (~22C) and light cycle (14:10
66 light:dark) and had *ad libitum* access to filtered tap water and a rat chow with minimal
67 phytoestrogens (Teklad 2019: Envigo, Indianapolis, IN). After acclimation, female rats were
68 observed for vaginal cytology indicating proestrus, and therefore receptivity. Receptive female
69 rats were randomly paired with an experienced breeder male, receptivity was confirmed, and the
70 pair was left together overnight. The following morning, vaginal cytology was checked for the
71 presence of sperm and if present marked as embryonic day (E1). The pregnant dams were single-
72 housed and provided nesting material on E18.

73 On E8, the dams (N = 6) were randomly split into two groups (each N = 3) and fed ¼ Nilla
74 Wafers™ with either 3% DMSO or 1 mg/kg Aroclor 1221 (A1221) (#C-221N, Accustandard, Lot
75 #072-202-01 - an estrogenic polychlorinated biphenol) from E8 – E18 and postnatal day (PND) 1

76 – 21. Treatment was not considered or analyzed in any of the data presented in this manuscript as
77 the goal was to first characterize the composition of EV sncRNAs, with greater statistical power
78 attained by combining the 6 litters. Treatment details are provided here for transparency. At PND
79 21, all pups were weaned and housed in cages of two or three. Only males were used in the present
80 manuscript and were otherwise unmanipulated until euthanasia besides weekly handling to
81 acclimate each rat to the experimenters in order to reduce stress. Females were used for other
82 projects.

83 **Sample Collection**

84 At PND 105, 6 male rats were randomly selected (N = 1 per litter) and euthanized by rapid
85 decapitation. The testis and epididymis were removed via a small incision in the scrotum. The
86 epididymis was separated from the testis and segmented into three portions (caput, corpus, and
87 cauda). The caput of the epididymis was minced into small pieces with scissors and placed in warm
88 (37 C) M2 culture media (M7167, Millipore Sigma) with HEPES and 2% exosome depleted fetal
89 bovine serum (A2720803, ThermoFisher). The slurry was placed on a rocker for 30 minutes to
90 allow sperm and epididymal fluid to suspend in solution, the supernatant was removed and large
91 tissue chunks were excluded. The resulting supernatant was centrifuged at 500 X g for 5 minutes
92 to pellet and remove sperm. The supernatant was again removed, immediately frozen on dry ice,
93 and stored at -80 C until use.

94 **Extracellular Vesicle Purification and Nucleic Acid Extraction**

95 The buffer supernatant containing extracellular vesicles from the caput of the epididymis
96 was thawed on ice for 30 minutes prior to isolation. After it was fully thawed the buffer was mixed
97 by pipetting and then filtered with a 0.8 um syringe filter (Millex-AA, SLAA033DD, Millipore
98 Sigma) to remove any cells or large cellular debris. Extracellular vesicles and RNA were
99 sequentially isolated from the media using the Qiagen exoRNeasy Midi kit (#77144, Qiagen,
100 Germantown, MD) according to the manufacturer's protocol. Briefly, 200 ul of media from each
101 sample was passed through a spin column that selectively binds exosomes. The column was

102 washed to remove contaminants and debris, and then eluted in Qiazol lysis buffer (#79306, Qiagen,
103 Germantown, MD). Chloroform (AAJ67241AP, FischerScientific) was added, mixed by shaking,
104 and incubated at room temperature to allow phase separation. Phase separation was aided by
105 centrifugation at 12,000 X g for 15 minutes at 4 C and the aqueous phase was aspirated and passed
106 through a second membrane spin column that selectively binds RNA. The membrane was washed
107 to remove contaminants and the sample eluted in 13 ul RNase free water. M2 culture media and
108 2% exosome depleted fetal bovine serum was used as a negative control to determine exogenous
109 contamination and subjected to the same extracellular vesicle and RNA isolation procedures
110 described above. These negative controls were analyzed via particle analysis and for resulting
111 nucleic acids to ensure there were no exogenous or contaminating exosomes or nucleic acids. None
112 were found.

113 **Extracellular Vesicle and RNA Quality Control**

114 An aliquot of the extracellular vesicles from the same samples described above were
115 isolated using the exoEasy Maxi Kit (76064, Qiagen) according to the manufacturer's protocols.
116 The resulting EVs from two samples were analyzed using a NanoSight 300 (Malvern Panalytical)
117 in 5 replicates to establish a size distribution of the resulting EVs and to ensure there were no
118 contaminating particles. RNA extracted from isolated EVs was first quantified (ND-1000,
119 ThermoScientific) and diluted for size distribution analysis and quality control using the small
120 RNA (5067-1548, Agilent) and pico RNA kits (5067-1514, Agilent) on a BioAnalyzer 2100
121 (Agilent). We found there was no cellular contamination indicated by a lack of 18s and 28s
122 ribosomal RNA and that the majority (~80%) of extracted RNA was in the 20-40 bp range,
123 indicative of small RNA molecules.

124 **Library Preparation, Sequencing, and Quality Control**

125 Library preparation was performed at the University of Texas Genomic Sequencing
126 Facility using the NEBNext Small RNA library preparation kit (E7330, New England
127 Biolabs). Samples were prepared with 14 cycles of PCR and the final product was size selected

128 using a 3% gel cassette on the Blue Pippin instrument (Sage Sciences), with the parameters set to
129 105-165 bp. Final size selected libraries were checked for quality on the Agilent BioAnalyzer with
130 High Sensitivity DNA analysis kit (5067-4626, Agilent) to confirm proper size selection. The
131 Kapa Library Quantification kit for Illumina libraries (KK4602) was used to determine the loading
132 concentrations prior to sequencing. Samples were sequenced on a NovaSeq 6000 Single Read,
133 SR50 run, with reads counts ranging from 25 to 32 million per sample.

134 **Analysis Pipeline**

135 Raw RNA reads were first passed through quality control (FastQC) and checked for read
136 quality and size distribution which showed excellent average read quality (avg. PHRED > 36) and
137 expected read length (50 bp). The raw reads were trimmed for Illumina adaptors (QuasR,
138 BioConductor) and again passed through quality control (FastQC) to determine per base read
139 quality and size distribution, which again showed excellent average read quality (avg. PHRED >
140 36) and an expected read length distribution (~30 nt) based on electrophoresis performed before
141 library prep. The trimmed reads were aligned (RBowtie, Bioconductor) to the unmasked rat
142 genome (Rnor v6) with strict matching parameters to ensure reads were aligned to best-hit
143 locations but were allowed multiple mapping locations (n = 12) due to the promiscuous nature of
144 small RNA origins. If the alignment parameters were met but a read mapped to multiple locations,
145 the read was randomly assigned to one of the similar best hit locations. Alignment efficiency was
146 analyzed for cross-species contamination or PCR primer amplification artifacts and was found to
147 be highly efficient (~85%). The aligned reads were assigned a feature annotation (Seqmonk, R,
148 BioConductor), visualized, and analyzed for read count and length distribution. Our annotation
149 pipeline considered reads aligned to microRNA (miRNA), piwi-interacting RNA (piRNA),
150 ribosomal RNA (rRNA), small nucleolar RNA (snoRNA), small nuclear RNA (snRNA), transfer
151 RNA (tRNA), long non-coding RNA (lncRNA), vault RNA, and YRNA. We also obtained
152 annotation tracks for nested and simple repeats (UCSC genome database) and microsatellites

153 (UCSC genome database). Reads were assigned an annotation designation only after considering
154 all other annotation types co-occurring in the same region.

155

156 **RESULTS**

157 **The size distribution of rat caput epididymosomes**

158 Particle tracking (NanoSight 300) was used to determine the size distribution of the
159 extracellular vesicles isolated from the caput of the rat epididymis using the Qiagen exoEasy Maxi
160 kit as described above. The isolated EVs from two separate samples were analyzed 5 times each.
161 The first sample had a mean EV size of 181.4 nm (SE 3), mode of 152 nm (SE 2.5), and standard
162 deviation of 40.6 nm (SE 1.1) and the second a mean of 178.7 (SE 0.5), mode of 156.1 (SE 3.8),
163 and standard deviation of 45.7 nm (SE 1.8). The size distribution and density of the extracellular
164 vesicles analyzed are shown in **Figure 1**. Approximately ~93% of all particles tracked were
165 between 50 and 250 nm in size, which are characteristic of epididymosomes [4].

166 **The small RNA contents of rat caput EVs**

167 The sncRNA contents of rat epididymosomes were dominated by reads that aligned to
168 tRNA (79.1%) or piRNA loci (18.1% - **Figure 2A**). We were surprised at the relatively low
169 abundance of miRNA in rats considering that mice models show substantial miRNA cargo in caput
170 epididymosomes [17]. All other annotation types, including miRNAs, accounted for the remaining
171 2.8% of the aligned reads. When tRNA and piRNA reads were removed from analysis and aligned
172 reads were analyzed as a proportion of the remaining reads (**Figure 2B**), the largest remaining
173 category belonged to reads that aligned to CpG islands (55.2%), which is not a known unit of
174 sncRNA expression (discussed below). The remaining reads aligned to YRNA (24.6%), lncRNA
175 (7.5%), miRNA (6.4%), rRNA (4.3%), and snoRNA (1.8%).

176 We analyzed the length of the reads aligned and assigned to each respective sncRNA
177 category to determine if our annotation pipeline performed well and to describe the subspecies of

178 various sncRNAs (**Table 1**). The two canonical categories with known read lengths were checked
179 first. The average read length for miRNA (22 nt) was exactly as expected and showed a 90-
180 percentile range of 19 – 27 nt. We set a cut-off of 10 reads per million (RPM) to determine which
181 miRNA were loaded into caput EVs and identified 15 miRNAs, the majority of which are known
182 to exist either in sperm or EVs in various models, and 5 uncharacterized miRNAs (**Table 2**).

183 We identified 81 piRNA loci that were substantially (> 10 RPM) expressed across the
184 genome, with clusters on chromosome 1, 2, 10, 13, 14 and 17. Approximately 60% (49/81) of the
185 expressed piRNA loci overlapped with known tRNA loci; these accounted for a significant portion
186 of all piRNA annotated reads (82.3%). These are a known subclass of piRNAs termed tRNA-
187 derived piRNA (td-piRNAs -- [36]) so we further analyzed their origin and determined that
188 virtually all of these reads aligned with the 5' end of tRNA loci (98.98%). Finally, we categorized
189 the tRNA type from which piRNAs were generated and determined that the majority were derived
190 from either 5'-tRNA^{Gly} (53.3%) or 5'-tRNA^{Glu} (32.6%) loci. 5'-tRNA^{Lys} (8.5%) and 5'-tRNA^{Val}
191 (2.3%) originating reads were also identified. The average read length for piRNA was also as
192 expected (30 nt) with a 90-precentile range of 26 – 32 nt.

193 **Small RNA fragments are prevalent in rat epididymosomes**

194 We then analyzed other sncRNA categories where read lengths can be variable depending
195 on how the RNA is processed. We found that reads aligned to tRNAs, which are ~70 – 100 nt [37],
196 had an average read length of 30 nt and a 90-precentile range of 28 – 31 nt (**Table 1**). This result
197 suggests that rat epididymosomes do not carry full length tRNAs, but rather carry either tRNA
198 fragments (tRFs) or tRNA-halves, which are 14 – 30 nt and 30 – 40 nt in length respectively [38].
199 We further categorized tRNA reads by aligning them to either the 5' or 3' end of a given tRNA
200 loci and discovered that 99.35% of all reads aligned to the 5' end (**Figure 3A**). Given their size
201 distribution, we were able to further categorize these reads. The tRNA reads show a 28 – 30 nt size
202 distribution indictive of tRF-5c fragments, the longest of the three known 5'-tRFs, or tRNA-halves
203 [39]. Alignment of reads to the tRNA structure (tRNAvis) confirmed their identity as tRF-5c

204 fragments because reads did not align to the anti-codon stem loop, which would be characteristic
205 of 5' tRNA-halves [38]. Because of the significant overlap of reads identified between piRNAs
206 and tRNA loci (presented above), we analyzed the proportion of tRNA reads that could be
207 accounted for by piRNA loci. We found that the majority tRNA reads (~81%) were unique to
208 tRNAs and could not be accounted for by overlapping piRNA loci. Finally, we analyzed the amino-
209 acid feature that tRNA reads were derived from and found that there was an over-representation
210 of reads derived from Glycine-tRNAs (81.4%). Reads were also found to originate from glutamate
211 (7.7%), histidine (6.9%), and lysine (1.7%) tRNA loci across the genome (**Figure 3B**). The size
212 distribution for 3' tRNA reads (**Figure 3C**) was similar but more broad compared to 5' tRNA
213 reads (**Figure 3D**).

214 We then looked at reads aligned to rRNA loci, which typically have a broad length range
215 depending on their rRNA type of origin (5s: ~120 nt [40], 5.8s: ~ 150 nt [41], 18s: 1874 nt [42],
216 and 28s: 4,802 nt [43]). In our samples, rRNAs had an average length of 22 nt and a 90-percentile
217 range of 17 – 31 nt (**Table 1**). These results suggest that rat caput epididymosomes do not carry
218 full length rRNA but instead carry rRNA fragments (rRFs). rRNA is expressed as a 45s pre-rRNA,
219 which contains the transcripts for 18s, 5.8s, and 28s rRNA, organized as cassettes of tandem
220 repeats on the short arms of chromosomes 3, 11, and 12 of the rat genome [44]. Reference genomes
221 are poorly annotated for these repeating cassettes because the number of repeats often varies
222 between individuals. Hence, these regions are typically masked in alignment reference genomes.
223 Nonetheless, there are a number of 5s rRNAs, which are expressed separately from the 45s pre-
224 rRNA, and 5.8s rRNA loci that are annotated in the rat reference genome that we analyzed.
225 Approximately 80% of rRNA derived reads aligned to 5.8s loci (**Figure 4A**). Subcategories of
226 rRFs have been described from human samples where short (18-19 nt), intermediate (24-25 nt),
227 and long (32-33 nt) rRFs are expressed depending on the rRNA type (e.g. 5s vs 5.8s) [45]. Our
228 data generally fit the categories described in human samples; 5s rRNA resulted in either short or
229 long transcripts (**Figure 4B**) whereas 5.8s rRNA resulted in intermediate fragments (**Figure 4C**).

230 Finally, we observed that the Y RNA was present in caput EVs at levels ~4 times that of
231 miRNA, which is surprising because we are not aware of any reports of Y RNA included in
232 epididymal EVs. Full length Y RNAs are ~80 – 110 nt in length [46]. We identified 13 (of 28) Y
233 RNA loci with substantial expression (> 10 RPKM). These reads demonstrated a sharp peak at 31
234 nt and a smaller peak at 22 nt with a 90-percentile range of 22 – 31 nt (**Table 1**). These results
235 suggest that rat caput EVs include fragments of Y RNA as a part of their sncRNA repertoire.

236 **Small RNA molecules are expressed from within CpG islands**

237 A subset of reads could not be accounted for by known and annotated sncRNA. We
238 identified dense clusters of expression that appeared to be expressed within the boundaries of GC-
239 rich CpG islands that were not fully accounted for by any other overlapping features (**Figure 5A**).
240 In total we found significant expression (>10 RPKM) within the boundaries of 50 CpG islands.
241 We visually inspected each of these CpG islands and were able to rule out the majority of them
242 due to overlapping features that had canonical expression patterns expected from features like
243 rRNA and piRNA (**Figure 5B**) or tRNA (**Figure 5C**). These loci were removed from further
244 analyses and the remaining 12 CpG islands were treated as an annotation category for sncRNAs.
245 We found this category to be the third most abundant behind tRNA and piRNA reads (**Figure 2A**
246 and **B**) and that the reads derived from CpG islands had a length distribution pattern that was
247 distinct from all of the other analyzed categories (**Figure 2C**) with a median length of 19 nt and a
248 90-percentile range of 15 – 28 nt (**Table 1**). As expected, the GC content of reads aligned to CpG
249 islands was substantial (~78%) compared to the average of all aligned reads (~50%).

250 We calculated a signal-to-noise ratio to determine if the reads we observed within CpG
251 islands were due to random chance [45]. When compared to the number of reads per kilobase
252 million (RPKM) over a 10 kb rolling window across the entire genome, our identified CpG islands
253 had a 609 s/n ratio. When compared to all CpG islands across the entire genome, our identified
254 CpG islands had a 92 s/n ratio. Put simply, the reads contained with our identified CpG islands
255 were 609 times more abundant than a random 10kb window in the genome and 92 times more

256 abundant than an average CpG island, indicating that the reads we observed were very unlikely to
257 be due to random chance.

258 Because CpG islands are not known units of small RNA expression, nor should they be
259 capable of such expression, we then tried to systematically demonstrate that the observed reads
260 were due to overlying features. We observed that CpG islands that contained more piRNA loci
261 appeared to be associated with more reads (**Figure 6A**), but when normalized for the read depth
262 and length of the CpG island (RPKM) the relationship was virtually non-existent ($R^2 = 0.077$,
263 **Table 3**). We quantified the reads that aligned under known piRNA loci and found that ~48% of
264 the total reads within the boundaries of CpG islands were also associated with piRNA loci.
265 However, we are hesitant to classify these reads as piRNA because they do not follow the canonical
266 length distribution associated with piRNA (~30nt) identified here and elsewhere [47]. None of the
267 reads (0.0%) within CpG islands were expressed from known tRNA loci. In a subset of the CpG
268 islands we observed, there was an abundance of predicted (eponine) transcriptional start sites
269 (**Figure 6B**), but this was not always the case (e.g. **Figure 5A**).

270 Finally, half (6/12) of the identified CpG islands were associated with annotated 5.8s rRNA
271 loci (**Table 3**). Functional rRNAs are expressed in tandem repeating cassettes that are processed
272 from a 45s precursor transcript that contains the functional 5.8s, 18s, and 28s rRNA after
273 processing. The rat genome is known to express these repeats from the short arms of chromosomes
274 3, 11, and 12 [44] on which none of our identified CpG islands reside. Notwithstanding, the rat
275 genome is poorly annotated for rRNA, so to overcome this shortcoming in the available
276 annotations we used BLAST to align the raw sequences expressed from CpG islands to the
277 available rRNA sequences: 45s, 32s (which includes the 28s rRNA and 5' sequence between the
278 transcription start site and 28s), 28s, 18s, and 5.8s. Approximately one third (~34.3%) of all reads
279 derived from CpG islands aligned to some form of rRNA or precursor rRNA. Of those reads that
280 aligned to any form of rRNA, the vast majority were derived from the 28s sequence (86.1% --
281 29.6% of all CpG island reads), while the 18s (11.15% -- 3.9% of all CpG island reads), and 5.8s
282 (0.16% -- 0.05% of all CpG island reads) accounted for a small proportion of the reads. The

283 remaining reads (2.6% -- 0.74% of all reads) aligned to the external or internal transcribed spacers
284 within the full length rRNA precursor transcript. In summary, while it appears that the CpG islands
285 we identified as expressing 19 nt small RNAs were in the vicinity of heretofore unannotated rRNA
286 or piRNA loci, the reads observed expressed within CpG islands cannot be fully accounted for by
287 either of these designations nor are their expression profiles congruent.

288 **DISCUSSION**

289 Epididymosomes from the caput are an essential component of sperm maturation and
290 acquisition of function [5,48,49]. They are also implicated in the control of heritable non-genetic
291 phenotypes, as their sncRNA cargo is altered by stress [19,22,25], diet [23,26,50], and alcohol
292 consumption [27]. Here, we provide the first comprehensive characterization of small RNAs
293 derived from caput EVs in the rat. We show that EVs isolated from the caput epididymis match
294 the size range of epididymosomes and that their small RNA contents are dominated by tRFs and
295 piRNA and contain far fewer miRNAs than expected from other organisms (Mice - [25,30,31],
296 Humans - [51]). We also identify Y RNA fragments in caput EVs for the first time in any organism,
297 although they are expressed in EVs of other organs [52–54]. Finally, we identify a potentially
298 novel small RNA molecule that is expressed from GC-rich CpG islands that cannot be accounted
299 for by known overlying small RNA features, and have a unique size distribution that is distinct
300 from other small RNAs analyzed.

301 **The sncRNA composition of rat caput EVs differs from that in mice**

302 The small RNA contents of EVs from the mouse caput epididymis are primarily miRNAs
303 (~60% - [25,30,31]), with over 350 expressed [17]. This is in contrast to the rat in which miRNAs
304 were a small portion (0.18%) of the small RNA complement. Of these, we identified 15 miRNAs,
305 7 of which overlapped with those in mice (miR-143, let-7c, let-7i, miR-26a, miR-99a, miR-143,
306 miR-148 [17]). The most abundant miRNA we identified in rats, miR-184, did not meet the
307 threshold for abundance in mice [17]. MiR-143, which is a hallmark of EVs in mice [17] and
308 humans [30], was also expressed in rats. There were also substantial species differences in tRFs,

309 which are the second most abundant category (~30%) in mouse caput EVs while piRNAs are
310 present at very low levels (<0.05% - [30,31]). Here, we show in rats that tRFs are by far the most
311 abundant category (~79%) and piRNAs are second most abundant (~18%). Further work is needed
312 to validate these findings and to understand why there are these dramatic species differences in the
313 EV sncRNA cargo.

314 **tRFs dominate the cargo of rat caput EVs**

315 tRFs, particularly from 5'-tRNA^{Gly} loci, dominated the cargo of caput EVs in the rat. As
316 sperm exit the testis, they contain few tRFs but their abundance gradually increases as sperm transit
317 from the proximal caput to the cauda [19,55]. In a mouse model, paternal diet changed the
318 abundance of 5'-tRF^{Gly} in sperm, which is implicated in the repression of endogenous
319 retroelements in pre-implantation embryos [19]. The authors suggested that EVs could deliver
320 these fragments, and we provide evidence that they are well poised to do so, and we confirmed the
321 exact species they identified (5'-tRF^{Gly}). We also identify 5'-tRF^{Glu} and 5'-tRF^{His} as prevalent in rat
322 caput EVs. The former (5'-tRF^{Glu}) has been implicated in playing a role in a high fat diet
323 intergenerational phenotype [26] via transcriptional regulation, directing alternate splicing, and
324 acetylation and phosphoprotein activation [27]. The latter (5'-tRF^{His}) has been implicated in
325 responses to low protein diets [19]. Further work is needed to elucidate their functional roles in
326 our rat model.

327 We found that tRFs in caput EVs are almost exclusively derived from the 5' end of tRNA
328 loci. There are two possible explanations for the overrepresentation of 5' tRFs. First, rat caput
329 epididymosomes may be selectively loaded with 5'-tRF fragments; these have actions similar to
330 RNA interference as governed by miRNAs, which act through the Argonaute pathway [56] to
331 silence endogenous retroelements in embryonic stem cells and embryos [19]. Alternatively, our
332 observation may be due to a technical bias in the sequencing library preparation procedure [38].
333 Libraries are amplified with PCR during preparation, which can be prematurely aborted if an RNA
334 molecule contains modified tRNA nucleobases that would be too short for sequencing, thereby

335 excluded, and not detected during analysis. In order to confirm the dominating presence of 5'-tRFs
336 in rat caput epididymosomes, a specific analysis pipeline (streamlined platform for observing
337 tRNA – SPOt) would need to be used to prevent observation bias [57].

338 **piRNAs are abundant and coincide with 5' tRNA fragments**

339 piRNAs represented a substantial proportion (18.1%) of EVs in the rat caput epididymis.
340 This is contrary to what is found in mouse models (< 0.05% -- [30,31]) but not entirely unexpected
341 as rat pachytene sperm are densely populated with piRNAs [58] depending on the stage of
342 development [59,60] presumably to control the expression of transposable elements in the
343 germline [61] by directing the catalyzation of de novo DNA methylation to suppress their
344 expression [62]. In the rat, unlike in the mouse, piRNAs appear poised to be delivered to sperm
345 via EVs in the caput epididymis. The reasons for this discrepancy between rats and mice could be
346 due to a number of reasons. First, this may represent a fundamental difference in the reproductive
347 biology between the two species. Second, it may be because the piRNAs that do exist in mouse
348 caput EVs are typically categorized as tRNA-halves instead of piRNA. We found that a majority
349 of reads that aligned with piRNA loci (~80%) also align to the 5' end of tRNA loci, which could
350 explain why they are missed during analysis in the mouse. The overlap of these two features
351 (piRNAs and tRFs) and expression from these loci has precedence. tRNA derived-piRNA (td-
352 piRNA) have been described in the testes of marmosets where Piwi proteins were found to bind
353 reads mapping to the 5'-tRNA^{Glu}, 5'-tRNA^{Gly}, and 5'-tRNA^{Val} loci [63]. It is intriguing that these
354 three identified td-piRNAs account for three of the four td-piRNAs found here and we believe we
355 are the first to identify these td-piRNA in a position poised to be delivered to sperm in the
356 epididymis. Additionally, we append 5'-tRNA^{Lys}, the third most abundant td-piRNA in our
357 analysis, as a potentially significant td-piRNA.

358 **rRNA fragments are present in three distinct sizes**

359 rRFs have long been considered RNA degradation or apoptotic by-products and have been
360 disregarded for any functional value. Compared to miRNA, piRNA, and tRFs, little is known about

361 the function or categories of rRFs and they have only recently been described [45] with nearly no
362 information existing in rats that we could find. Interestingly, rRFs appear in immunoprecipitations
363 with the Argonaute complex in mice and humans, which suggests a role for translational regulation
364 [64]. In humans, three distinct categories of rRFs are known with differential expression in each
365 of the rRNA categories (e.g. 5s, 5.8s, 18s, and 28s); short (18-21 nt), intermediate (24-25 nt), and
366 long (26-33 nt) [45]. Our ability to map rRFs to the reference genome was limited by the lack of
367 annotations for rRNA in the rat genome, but given the annotations we did have, we identified a
368 similar expression profile to Cherlin et al. (2020) (in human samples -- [45]) in which three distinct
369 subtypes of rRFs were present: 18 nt & 30 nt rRFs originating from 5s loci and 22 nt rRFs from
370 5.8s loci. Furthermore, rRFs are sparsely reported in reproductive tissue (Humans -- [65,66],
371 Bovine -- [67]) and we believe we are the first to report their presence in caput EV samples, which
372 suggests a novel role for rRFs in reproduction.

373 **19-nt small RNAs are expressed from within the boundaries of CpG Islands**

374 There were 12 identified loci in the rat genome that corresponded with substantial
375 expression of 19-nt small RNAs that are GC rich and expressed within the boundaries of annotated
376 CpG islands. We postulate that this is a novel unit of expression for sncRNAs. CpG islands are
377 generally annotated based on the characteristics of their sequence; longer than 200-bp with a GC
378 content higher than 50% and an expected to observed ratio greater than 0.6 [68]. Many of the first
379 CpG islands were identified at the 5' end of "housekeeping" genes [69,70] but have since been
380 computationally and experimentally predicted across the genome, including in inter- and
381 intragenic space [71]. Parts of CpG islands are sometimes transcribed on the 5' or 3' end of
382 expressed genes and removed during splicing unless they extend into an exon, including sncRNAs
383 [71,72]. This expression pattern we observed within CpG islands does not appear to have a
384 relationship with any other annotation type; although we considered other nearby or overlying
385 rRNA cassettes or piRNA clusters, neither accounted for all of the reads or loci, and some loci had
386 neither feature. Nevertheless, we carefully inspected the involvement of both types of features.

387 For rRNAs, it is difficult to determine the precise location of cassettes because they are not
388 well annotated in the rat genome. By using sequence similarity via BLAST alignment, we
389 determined that ~34% of the small RNA expressed from CpG islands are found within the 45s pre-
390 rRNA transcript, the majority of those from the 28s sequence (~86%). Because of their 19 nt
391 length, we can say with certainty these reads are not from mature rRNAs. Furthermore, we are
392 hesitant to term these rRNA fragments for two reasons; first, the length of the reads (19 nt) from
393 annotated 5.8s rRNA within the identified CpG islands do not correspond to other 5.8s rRNA reads
394 (22 nt) found elsewhere in this data set; and second, the expression profile of the 19 nt reads are
395 bounded by the CpG island and not by the 5.8s rRNA or predicted position of 45s rRNA. It is
396 possible that the observed CpG islands may be a part of the ~30 kb non-transcribed spacer that
397 separates 45s repeats, but as the name implies, these portions are up or downstream of rRNA and
398 should not be transcribed.
399 A second possibility is that the reads we identified arise from piRNA clusters. The function
400 of piRNA is RNA-guided silencing mediated by Piwi proteins (Riwi in the rat) that are particularly
401 active in the germline of the testes [73,74]. piRNAs regulate the expression of transposable
402 elements [59,75] by inducing de novo DNA methylation [76]. Primary piRNA can be amplified
403 by "ping-pong amplification" [77] by binding to expressed transposable elements which are
404 cleaved to generate a secondary guide transcript that ensure the lack of transposition [59,78].
405 Primary piRNA are observed in developing germ cells [76] while secondary piRNAs, generated
406 by the ping-pong cycle, are thought only to be present before pachytene stages in the basal
407 compartment of the testes [59,76] after which only primary piRNAs should be present [76,79].
408 The transcripts we identified in caput EVs are well outside of the window of canonical piRNA
409 functionality and while they appear to be associated with piRNA clusters, when read depth is
410 corrected for by the length of a CpG island the association becomes non-existent. Furthermore,
411 their distinct 19-nt signature differentiates them from canonical piRNAs which are typically 26-
412 35 nt in length [80].

413 A final possibility we considered is that the 19-nt sRNA we observe are byproducts from
414 the generation of secondary piRNAs during which exonuclease activity should generate fragments
415 of a consistent size due to the portion of the transcript that is shielded by Piwi-complex itself [76].
416 There have been three reports we could find that have identified such byproducts [81–83].
417 Berninger et al. (2011) were the first to identify "19mers" expressed from both the sense and anti-
418 sense strands of piRNA clusters solely in the testis of rats, mice, and platypuses, but did not find
419 them in any other tissue type [81]. Oey et al. (2011) also described 19mer byproducts of piRNA
420 with a focus on repeat elements (LINEs, SINEs, LTRs) and IAPs where ping-pong amplification
421 is predicted [82]. They also found that 19mers that were equally present from both the sense and
422 antisense strands, were exclusive to the testes, and while they didn't specifically analyze or
423 mention it, their data show no GC content bias. Ichiyanagi et al. (2014) also observed 19mers
424 immediately upstream of piRNAs but dismissed them as piRNA amplification byproducts as per
425 Berninger et al. and Oey et al. (2011) [83]. The commonality of the piRNA amplification
426 byproducts identified in these reports is that they are 19nt fragments expressed from a broad
427 distribution on both strands relative to the piRNA cluster, a profile that does not fit our current
428 observation.

429 Based on this evidence, we do not believe that the alternatives (rRNA fragments,
430 piRNAs, or piRNA amplification byproducts) can account for our observation of GC-rich 19-nt
431 small RNAs. These "CpG island small RNAs" extend outside of the boundaries of annotated rRNA
432 and piRNA, which account for only a portion of the observations, and do not abide by their
433 respective canonical length characteristics. It is also possible that these observations could be the
434 19mer byproduct of piRNA amplification observed elsewhere [81–83] but there are 3 reasons we
435 do not think this is likely. First, we observe these reads in extracellular vesicles while the

436 byproducts of piRNA amplification are known only to exist in pre-pachytene spermatocytes and
437 should be derived from both the sense and anti-sense strands, a characteristic we do not see. If this
438 observation is due to 19mer piRNA amplification byproducts generated in the epididymis, then
439 our data provide functional significance to their existence not previously reported. Second, the
440 reads we observe are expressly within the boundaries of CpG islands with a GC content not
441 reported elsewhere. The specificity of the expression loci, and the lack of high GC content in other
442 reports make their identity as byproducts unlikely. Finally, we observe expression from multiple
443 CpG islands not linked with known piRNA loci. If these are indeed the byproduct of piRNA
444 amplification, our data then represent the identification of novel piRNA loci that would seem to
445 be important for the final steps of sperm maturation. Mature sperm transiting the epididymis should
446 be transcriptionally quiescent [84–87], and therefore transposons should not be expressed.
447 Ascertaining a functional role of these small RNAs requires further investigation.

448 **Conclusions**

449 EVs from the rat caput epididymis carry a complex repertoire of small RNAs and their
450 contents are substantially different from the mouse. The dominant features we identify are tRNA
451 fragments and piRNAs derived from tRNA loci. MicroRNAs are poorly represented in stark
452 contrast to mice. We also identify two types of small RNA not previously seen in caput EVs, rRNA
453 fragments and Y RNA fragments, and described a potentially novel small RNA we have termed
454 CpG island (CpGi) sRNAs. These data represent an exciting collection of possibilities for future
455 researchers studying basic reproductive biology and the complexities of epigenetic
456 transgenerational inheritance.

Conflict of Interest: The authors declare no conflict of interest.

Grant funding: Supported by and RO1 ES029464 to A.C.G. and PhRMA Foundation Postdoctoral Fellowship to R.G.

Acknowledgement: The authors recognize Mandee Bell and Lindsay M. Thompson for their assistance with animal husbandry, treatment, and sample collection. We would also like to acknowledge the excellent work (small RNA library preparation and sequencing) performed by the Genomic Sequencing and Analysis Facility at UT Austin, Center for Biomedical Research Support. RRID#: SCR_021713.

462 **REFERENCES**
463

464 1. Hermo, L.; Pelletier, R. ‐ Marc; Cyr, D.G.; Smith, C.E. Surfing the Wave, Cycle, Life
465 History, and Genes/Proteins Expressed by Testicular Germ Cells. Part 1: Background to
466 Spermatogenesis, Spermatogonia, and Spermatocytes. *Microsc Res Techniq* 2010, *73*, 241–278,
467 doi:10.1002/jemt.20783.

468 2. Cornwall, G.A. New Insights into Epididymal Biology and Function. *Hum Reprod Update*
469 2009, *15*, 213–227, doi:10.1093/humupd/dmn055.

470 3. Sullivan, R.; Saez, F. Epididymosomes, Prostasomes, and Liposomes: Their Roles in
471 Mammalian Male Reproductive Physiology. *Reproduction* 2001, *146*, R21–R35,
472 doi:10.1530/rep-13-0058.

473 4. Sullivan, R. Epididymosomes: A Heterogeneous Population of Microvesicles with Multiple
474 Functions in Sperm Maturation and Storage. *Asian J Androl* 2015, *0*, 0, doi:10.4103/1008-
475 682x.155255.

476 5. Martin-DeLeon, P.A. Epididymosomes: Transfer of Fertility-Modulating Proteins to the
477 Sperm Surface. *Asian J Androl* 2015, *17*, 720–725, doi:10.4103/1008-682x.155538.

478 6. Martin-DeLeon, P.A. Epididymal SPAM1 and Its Impact on Sperm Function. *Mol Cell*
479 *Endocrinol* 2006, *250*, 114–121, doi:10.1016/j.mce.2005.12.033.

480 7. Fornés, M.W.; Barbieri, A.; Cavicchia, J.C. Morphological and Enzymatic Study of
481 Membrane ‐ bound Vesicles from the Lumen of the Rat Epididymis. *Andrologia* 1995, *27*, 1–5,
482 doi:10.1111/j.1439-0272.1995.tb02087.x.

483 8. Rejraji, H.; Sion, B.; Prensier, G.; Carreras, M.; Motta, C.; Frenoux, J.-M.; Vericel, E.;
484 Grizard, G.; Vernet, P.; Drevet, J.R. Lipid Remodeling of Murine Epididymosomes and
485 Spermatozoa During Epididymal Maturation. *Biol Reprod* 2006, *74*, 1104–1113,
486 doi:10.1095/biolreprod.105.049304.

487 9. Grimalt, P.; Bertini, F.; Fornes, M.W. HIGH-AFFINITY SITES FOR Beta-D-
488 GALACTOSIDASE ON MEMBRANE-BOUND VESICLES ISOLATED FROM RAT
489 EPIDIDYMAL FLUID. *Arch Andrology* 2009, *44*, 85–91, doi:10.1080/014850100262245.

490 10. Hermo, L.; Jacks, D. Nature's Ingenuity: Bypassing the Classical Secretory Route via
491 Apocrine Secretion. *Mol Reprod Dev* 2002, *63*, 394–410, doi:10.1002/mrd.90023.

492 11. Oh, J.S.; Han, C.; Cho, C. ADAM7 Is Associated with Epididymosomes and Integrated into
493 Sperm Plasma Membrane. *Mol Cells* 2009, *28*, 441–446, doi:10.1007/s10059-009-0140-x.

494 12. Zhou, W.; Iuliis, G.N.D.; Dun, M.D.; Nixon, B. Characteristics of the Epididymal Luminal
495 Environment Responsible for Sperm Maturation and Storage. *Front Endocrinol* 2018, *9*, 59,
496 doi:10.3389/fendo.2018.00059.

497 13. Frenette, G.; Lessard, C.; Sullivan, R. Polyol Pathway along the Bovine Epididymis. *Mol*
498 *Reprod Dev* 2004, *69*, 448–456, doi:10.1002/mrd.20170.

499 14. Sutovsky, P.; Moreno, R.; Ramalho-Santos, J.; Dominko, T.; Thompson, W.E.; Schatten, G.
500 A Putative, Ubiquitin-Dependent Mechanism for the Recognition and Elimination of Defective
501 Spermatozoa in the Mammalian Epididymis. *J Cell Sci* 2001, *114*, 1665–1675,
502 doi:10.1242/jcs.114.9.1665.

503 15. D'Amours, O.; Frenette, G.; Bordeleau, L.-J.; Allard, N.; Leclerc, P.; Blondin, P.; Sullivan,
504 R. Epididymosomes Transfer Epididymal Sperm Binding Protein 1 (ELSPBP1) to Dead
505 Spermatozoa During Epididymal Transit in Bovine1. *Biol Reprod* 2012, *87*, Article 94, 1-11,
506 doi:10.1095/biolreprod.112.100990.

507 16. Belleanne, C.; Calvo, zequiel; Caballero, J.; Sullivan, R. Epididymosomes Convey Different
508 Repertoires of MicroRNAs Throughout the Bovine Epididymis1. *Biol Reprod* 2013, *89*, Article
509 30, 1-11, doi:10.1095/biolreprod.113.110486.

510 17. Reilly, J.N.; McLaughlin, E.A.; Stanger, S.J.; Anderson, A.L.; Hutcheon, K.; Church, K.;
511 Mihalas, B.P.; Tyagi, S.; Holt, J.E.; Eamens, A.L.; et al. Characterisation of Mouse
512 Epididymosomes Reveals a Complex Profile of MicroRNAs and a Potential Mechanism for
513 Modification of the Sperm Epigenome. *Sci Rep-uk* 2016, *6*, 31794, doi:10.1038/srep31794.

514 18. Caballero, J.N.; Frenette, G.; Belleannée, C.; Sullivan, R. CD9-Positive Microvesicles
515 Mediate the Transfer of Molecules to Bovine Spermatozoa during Epididymal Maturation. *Plos*
516 *One* 2013, *8*, e65364, doi:10.1371/journal.pone.0065364.

517 19. Sharma, U.; Conine, C.C.; Shea, J.M.; Boskovic, A.; Derr, A.G.; Bing, X.Y.; Belleannee, C.;
518 Kucukural, A.; Serra, R.W.; Sun, F.; et al. Biogenesis and Function of TRNA Fragments during
519 Sperm Maturation and Fertilization in Mammals. *Science* 2016, *351*, 391,
520 doi:10.1126/science.aad6780.

521 20. Conine, C.C.; Sun, F.; Song, L.; Rivera-Pérez, J.A.; Rando, O.J. Small RNAs Gained during
522 Epididymal Transit of Sperm Are Essential for Embryonic Development in Mice. *Dev Cell* 2018,
523 *46*, 470-480.e3, doi:10.1016/j.devcel.2018.06.024.

524 21. Suryawanshi, A.R.; Khan, S.A.; Joshi, C.S.; Khole, V.V. Epididymosome‐Mediated
525 Acquisition of MMSDH, an Androgen‐Dependent and Developmentally Regulated Epididymal
526 Sperm Protein. *J Androl* 2012, *33*, 963–974, doi:10.2164/jandrol.111.014753.

527 22. Rodgers, A.B.; Morgan, C.P.; Bronson, S.L.; Revello, S.; Bale, T.L. Paternal Stress Exposure
528 Alters Sperm MicroRNA Content and Reprograms Offspring HPA Stress Axis Regulation. *J*
529 *Neurosci* 2013, *33*, 9003--9012, doi:10.1523/jneurosci.0914-13.2013.

530 23. Chen, Q.; Yan, M.; Cao, Z.; Li, X.; Zhang, Y.; Shi, J.; Feng, G.; Peng, H.; Zhang, X.; Zhang,
531 Y.; et al. Sperm TsRNAs Contribute to Intergenerational Inheritance of an Acquired Metabolic
532 Disorder. *Science* 2016, *351*, 397, doi:10.1126/science.aad7977.

533 24. Fullston, T.; Teague, E.M.C.O.; Palmer, N.O.; DeBlasio, M.J.; Mitchell, M.; Corbett, M.;
534 Print, C.G.; Owens, J.A.; Lane, M. Paternal Obesity Initiates Metabolic Disturbances in Two
535 Generations of Mice with Incomplete Penetrance to the F2 Generation and Alters the
536 Transcriptional Profile of Testis and Sperm MicroRNA Content. *Faseb J* 2013, *27*, 4226–4243,
537 doi:10.1096/fj.12-224048.

538 25. Short, A.; Fennell, K.; Perreau, V.; Fox, A.; O'Bryan, M.; Kim, J.H.; Bredy, T.; Pang, T.;
539 Hannan, A. Elevated Paternal Glucocorticoid Exposure Alters the Small Noncoding RNA Profile
540 in Sperm and Modifies Anxiety and Depressive Phenotypes in the Offspring. *Translational*
541 *Psychiatry* 2016, *6*.

542 26. Barbosa, T. de C.; Ingerslev, L.R.; Alm, P.S.; Versteyhe, S.; Massart, J.; Rasmussen, M.;
543 Donkin, I.; Sjögren, R.; Mudry, J.M.; Vetterli, L.; et al. High-Fat Diet Reprograms the
544 Epigenome of Rat Spermatozoa and Transgenerationally Affects Metabolism of the Offspring.
545 *Mol Metab* 2015, *5*, 184–197, doi:10.1016/j.molmet.2015.12.002.

546 27. Rompala, G.R.; Mounier, A.; Wolfe, C.M.; Lin, Q.; Lefterov, I.; Homanics, G.E. Heavy
547 Chronic Intermittent Ethanol Exposure Alters Small Noncoding RNAs in Mouse Sperm and
548 Epididymosomes. *Frontiers Genetics* 2018, *9*, 32–32, doi:10.3389/fgene.2018.00032.

549 28. Gapp, K.; Jawaid, A.; Sarkies, P.; Bohacek, J.; Pelczar, P.; Prados, J.; Farinelli, L.; Miska, E.;
550 Mansuy, I.M. Implication of Sperm RNAs in Transgenerational Inheritance of the Effects of
551 Early Trauma in Mice. *Nat Neurosci* 2014, *17*, 667–669, doi:10.1038/nn.3695.

552 29. Chan, J.C.; Morgan, C.P.; Leu, N.A.; Shetty, A.; Cisse, Y.M.; Nugent, B.M.; Morrison, K.E.;
553 Jašarević, E.; Huang, W.; Kanyuch, N.; et al. Reproductive Tract Extracellular Vesicles Are
554 Sufficient to Transmit Intergenerational Stress and Program Neurodevelopment. *Nat Commun*
555 2020, *11*, 1499, doi:10.1038/s41467-020-15305-w.

556 30. Trigg, N.A.; Eamens, A.L.; Nixon, B. The Contribution of Epididymosomes to the Sperm
557 Small RNA Profile. *Reproduction* 2019, *1*, R209–R223, doi:10.1530/rep-18-0480.

558 31. Hutcheon, K.; McLaughlin, E.A.; Stanger, S.J.; Bernstein, I.R.; Dun, M.D.; Eamens, A.L.;
559 Nixon, B. Analysis of the Small Non-Protein-Coding RNA Profile of Mouse Spermatozoa
560 Reveals Specific Enrichment of PiRNAs within Mature Spermatozoa. *Rna Biol* 2017, *14*, 1776–
561 1790, doi:10.1080/15476286.2017.1356569.

562 32. Wei, H.; Zhou, B.; Zhang, F.; Tu, Y.; Hu, Y.; Zhang, B.; Zhai, Q. Profiling and Identification
563 of Small RDNA-Derived RNAs and Their Potential Biological Functions. *Plos One* 2013, *8*,
564 e56842, doi:10.1371/journal.pone.0056842.

565 33. Wei, Y.; Schatten, H.; Sun, Q.-Y. Environmental Epigenetic Inheritance through Gametes
566 and Implications for Human Reproduction. *Hum Reprod Update* 2015, *21*, 194–208,
567 doi:10.1093/humupd/dmu061.

568 34. Ellenbroek, B.; Youn, J. Rodent Models in Neuroscience Research: Is It a Rat Race? *Dis*
569 *Model Mech* 2016, *9*, 1079–1087, doi:10.1242/dmm.026120.

570 35. Burns, S.B.; Szyszkowicz, J.K.; Luheshi, G.N.; Lutz, P.-E.; Turecki, G. Plasticity of the
571 Epigenome during Early-Life Stress. *Semin Cell Dev Biol* 2018, *77*, 115–132,
572 doi:10.1016/j.semcdb.2017.09.033.

573 36. Honda, S.; Kawamura, T.; Loher, P.; Morichika, K.; Rigoutsos, I.; Kirino, Y. The Biogenesis
574 Pathway of TRNA-Derived PiRNAs in Bombyx Germ Cells. *Nucleic Acids Res* 2017, *45*, 9108–
575 9120, doi:10.1093/nar/gkx537.

576 37. Krahn, N.; Fischer, J.T.; Söll, D. Naturally Occurring TRNAs With Non-Canonical
577 Structures. *Front Microbiol* 2020, *11*, 596914, doi:10.3389/fmicb.2020.596914.

578 38. Shen, Y.; Yu, X.; Zhu, L.; Li, T.; Yan, Z.; Guo, J. Transfer RNA-Derived Fragments and
579 TRNA Halves: Biogenesis, Biological Functions and Their Roles in Diseases. *J Mol Med* 2018,
580 *96*, 1167–1176, doi:10.1007/s00109-018-1693-y.

581 39. Kumar, P.; Anaya, J.; Mudunuri, S.B.; Dutta, A. Meta-Analysis of TRNA Derived RNA
582 Fragments Reveals That They Are Evolutionarily Conserved and Associate with AGO Proteins
583 to Recognize Specific RNA Targets. *Bmc Biol* 2014, *12*, 78, doi:10.1186/s12915-014-0078-0.

584 40. Gray, M.W.; Burger, G.; Lang, B.F. Mitochondrial Evolution. *Science* 1999, *283*, 1476–
585 1481, doi:10.1126/science.283.5407.1476.

586 41. Walker, T.A.; Pace, N.R. 5.8S Ribosomal RNA. *Cell* 1983, *33*, 320–322, doi:10.1016/0092-
587 8674(83)90413-0.

588 42. Chan, Y.L.; Gutell, R.; Noller, H.F.; Wool, I.G. The Nucleotide Sequence of a Rat 18 S
589 Ribosomal Ribonucleic Acid Gene and a Proposal for the Secondary Structure of 18 S
590 Ribosomal Ribonucleic Acid. *J Biol Chem* 1984, *259*, 224–230, doi:10.1016/s0021-
591 9258(17)43645-3.

592 43. Hadjiolov, A.A.; Georgiev, O.I.; Nosikov, V.V.; Yavachev, L.P. Primary and Secondary
593 Structure of Rat 28 S Ribosomal RNA. *Nucleic Acids Res* 1984, *12*, 3677–3693,
594 doi:10.1093/nar/12.8.3677.

595 44. Sasaki, M.; Nishida, C.; Kodama, Y. Characterization of Silver-Stained Nucleolus Organizer
596 Regions (Ag-NORs) in 16 Inbred Strains of the Norway Rat, Rattus Norvegicus. *Cytogenet*
597 *Genome Res* 1986, *41*, 83–88, doi:10.1159/000132208.

598 45. Cherlin, T.; Magee, R.; Jing, Y.; Pliatsika, V.; Loher, P.; Rigoutsos, I. Ribosomal RNA
599 Fragmentation into Short RNAs (RRFs) Is Modulated in a Sex- and Population of Origin-
600 Specific Manner. *Bmc Biol* 2020, *18*, 38, doi:10.1186/s12915-020-0763-0.

601 46. Wolin, S.L.; Steitz, J.A. Genes for Two Small Cytoplasmic Ro RNAs Are Adjacent and
602 Appear to Be Single-Copy in the Human Genome. *Cell* 1983, *32*, 735–744, doi:10.1016/0092-
603 8674(83)90059-4.

604 47. Beyret, E.; Liu, N.; Lin, H. PiRNA Biogenesis during Adult Spermatogenesis in Mice Is
605 Independent of the Ping-Pong Mechanism. *Cell Res* 2012, *22*, 1429–1439,
606 doi:10.1038/cr.2012.120.

607 48. Sullivan, R.; Frenette, G.; Girouard, J. Epididymosomes Are Involved in the Acquisition of
608 New Sperm Proteins during Epididymal Transit. *Asian J Androl* 2007, *9*, 483–491,
609 doi:10.1111/j.1745-7262.2007.00281.x.

610 49. Caballero, J.; Frenette, G.; D'Amours, O.; Belleannée, C.; Lacroix‐Pepin, N.; Robert, C.;
611 Sullivan, R. Bovine Sperm Raft Membrane Associated Glioma Pathogenesis‐Related 1‐like
612 Protein 1 (GliPr1L1) Is Modified during the Epididymal Transit and Is Potentially Involved in
613 Sperm Binding to the Zona Pellucida. *J Cell Physiol* 2012, *227*, 3876–3886,
614 doi:10.1002/jcp.24099.

615 50. Fullston, T.; Teague, E.M.C.O.; Palmer, N.O.; DeBlasio, M.J.; Mitchell, M.; Corbett, M.;
616 Print, C.G.; Owens, J.A.; Lane, M. Paternal Obesity Initiates Metabolic Disturbances in Two
617 Generations of Mice with Incomplete Penetrance to the F2 Generation and Alters the
618 Transcriptional Profile of Testis and Sperm MicroRNA Content. *The FASEB Journal* 2013, *27*,
619 4226–4243.

620 51. Belleannée, C.; Calvo, E.; Thimon, V.; Cyr, D.G.; Légaré, C.; Garneau, L.; Sullivan, R. Role
621 of MicroRNAs in Controlling Gene Expression in Different Segments of the Human Epididymis.
622 *Plos One* 2012, *7*, e34996, doi:10.1371/journal.pone.0034996.

623 52. Kowalski, M.P.; Krude, T. Functional Roles of Non-Coding Y RNAs. *Int J Biochem Cell*
624 *Biology* 2015, *66*, 20–29, doi:10.1016/j.biocel.2015.07.003.

625 53. Driedonks, T.A.P.; Hoen, E.N.M.N.-'t Circulating Y-RNAs in Extracellular Vesicles and
626 Ribonucleoprotein Complexes; Implications for the Immune System. *Front Immunol* 2019, *9*,
627 3164, doi:10.3389/fimmu.2018.03164.

628 54. Driedonks, T.A.P.; Mol, S.; Bruin, S. de; Peters, A.-L.; Zhang, X.; Lindenbergh, M.F.S.;
629 Beuger, B.M.; Stalborch, A.-M.D. van; Spaan, T.; Jong, E.C. de; et al. Y-RNA Subtype Ratios in
630 Plasma Extracellular Vesicles Are Cell Type- Specific and Are Candidate Biomarkers for
631 Inflammatory Diseases. *J Extracell Vesicles* 2020, *9*, 1764213,
632 doi:10.1080/20013078.2020.1764213.

633 55. Stanger, S.J.; Bernstein, I.R.; Anderson, A.L.; Hutcheon, K.; Dun, M.D.; Eamens, A.L.;
634 Nixon, B. The Abundance of a Transfer RNA-Derived RNA Fragment Small RNA
635 Subpopulation Is Enriched in Cauda Spermatozoa. *Exrna* 2020, *2*, 17, doi:10.1186/s41544-020-
636 00058-x.

637 56. Gagnon, K.T.; Corey, D.R. Argonaute and the Nuclear RNAs: New Pathways for RNA-
638 Mediated Control of Gene Expression. *Nucleic Acid Ther* 2012, *22*, 3–16,
639 doi:10.1089/nat.2011.0330.

640 57. Grelet, S.; McShane, A.; Hok, E.; Tomberlin, J.; Howe, P.H.; Geslain, R. SPOt: A Novel and
641 Streamlined Microarray Platform for Observing Cellular TRNA Levels. *Plos One* 2017, *12*,
642 e0177939, doi:10.1371/journal.pone.0177939.

643 58. Stermer, A.R.; Reyes, G.; Hall, S.J.; Boekelheide, K. Small RNAs in Rat Sperm Are a
644 Predictive and Sensitive Biomarker of Exposure to the Testicular Toxicant Ethylene Glycol
645 Monomethyl Ether. *Toxicol Sci* 2019, *169*, 399–408, doi:10.1093/toxsci/kfz041.

646 59. Aravin, A.A.; Sachidanandam, R.; Girard, A.; Fejes-Toth, K.; Hannon, G.J. Developmentally
647 Regulated PiRNA Clusters Implicate MILI in Transposon Control. *Science* 2007, *316*, 744–747,
648 doi:10.1126/science.1142612.

649 60. Smorag, L.; Zheng, Y.; Nolte, J.; Zechner, U.; Engel, W.; Pantakani, D.V.K. MicroRNA
650 Signature in Various Cell Types of Mouse Spermatogenesis: Evidence for Stage‐specifically
651 Expressed MiRNA‐221, ‐203 and ‐34b‐5p Mediated Spermatogenesis Regulation. *Biol*
652 *Cell* 2012, *104*, 677–692, doi:10.1111/boc.201200014.

653 61. Newkirk, S.J.; Lee, S.; Grandi, F.C.; Gaysinskaya, V.; Rosser, J.M.; Berg, N.V.; Hogarth,
654 C.A.; Marchetto, M.C.N.; Muotri, A.R.; Griswold, M.D.; et al. Intact PiRNA Pathway Prevents
655 L1 Mobilization in Male Meiosis. *Proc National Acad Sci* 2017, *114*, E5635–E5644,
656 doi:10.1073/pnas.1701069114.

657 62. Peng, J.C.; Lin, H. Beyond Transposons: The Epigenetic and Somatic Functions of the Piwi-
658 PiRNA Mechanism. *Curr Opin Cell Biol* 2013, *25*, 190–194, doi:10.1016/j.ceb.2013.01.010.

659 63. Hirano, T.; Iwasaki, Y.W.; Lin, Z.Y.-C.; Imamura, M.; Seki, N.M.; Sasaki, E.; Saito, K.;
660 Okano, H.; Siomi, M.C.; Siomi, H. Small RNA Profiling and Characterization of PiRNA
661 Clusters in the Adult Testes of the Common Marmoset, a Model Primate. *Rna* 2014, *20*, 1223–
662 1237, doi:10.1261/rna.045310.114.

663 64. Guan, L.; Grigoriev, A. Computational Meta-Analysis of Ribosomal RNA Fragments:
664 Potential Targets and Interaction Mechanisms. *Nucleic Acids Res* 2021, *49*, gkab190-,
665 doi:10.1093/nar/gkab190.

666 65. Goodrich, R.J.; Anton, E.; Krawetz, S.A. Spermatogenesis, Methods and Protocols. *Methods*
667 *Mol Biology* 2012, 385–396, doi:10.1007/978-1-62703-038-0_33.

668 66. Johnson, G.D.; Sendler, E.; Lalancette, C.; Hauser, R.; Diamond, M.P.; Krawetz, S.A.
669 Cleavage of RRNA Ensures Translational Cessation in Sperm at Fertilization. *Mhr Basic Sci*
670 *Reproductive Medicine* 2011, *17*, 721–726, doi:10.1093/molehr/gar054.

671 67. Almiñana, C.; Tsikis, G.; Labas, V.; Uzbekov, R.; Silveira, J.C. da; Bauersachs, S.;
672 Mermillod, P. Deciphering the Oviductal Extracellular Vesicles Content across the Estrous
673 Cycle: Implications for the Gametes-Oviduct Interactions and the Environment of the Potential
674 Embryo. *Bmc Genomics* 2018, *19*, 622, doi:10.1186/s12864-018-4982-5.

675 68. Gardiner-Garden, M.; Frommer, M. CpG Islands in Vertebrate Genomes. *J Mol Biol* 1987,
676 *196*, 261–282, doi:10.1016/0022-2836(87)90689-9.

677 69. Cooper, D.N.; Gerber-Huber, S. DNA Methylation and CpG Suppression. *Cell Differ Dev*
678 1985, *17*, 199–205, doi:10.1016/0045-6039(85)90488-9.

679 70. Bird, A.P. CpG-Rich Islands and the Function of DNA Methylation. *Nature* 1986, *321*, 209–
680 213, doi:10.1038/321209a0.

681 71. Medvedeva, Y.A.; Fridman, M.V.; Oparina, N.J.; Malko, D.B.; Ermakova, E.O.;
682 Kulakovskiy, I.V.; Heinzel, A.; Makeev, V.J. Intergenic, Gene Terminal, and Intragenic CpG
683 Islands in the Human Genome. *Bmc Genomics* 2010, *11*, 48–48, doi:10.1186/1471-2164-11-48.

684 72. Hackenberg, M.; Previti, C.; Luque-Escamilla, P.L.; Carpena, P.; Martínez-Aroza, J.; Oliver,
685 J.L. CpGcluster: A Distance-Based Algorithm for CpG-Island Detection. *Bmc Bioinformatics*
686 2006, *7*, 446–446, doi:10.1186/1471-2105-7-446.

687 73. Aravin, A.; Gaidatzis, D.; Pfeffer, S.; Lagos-Quintana, M.; Landgraf, P.; Iovino, N.; Morris,
688 P.; Brownstein, M.J.; Kuramochi-Miyagawa, S.; Nakano, T.; et al. A Novel Class of Small
689 RNAs Bind to MILI Protein in Mouse Testes. *Nature* 2006, *442*, 203–207,
690 doi:10.1038/nature04916.

691 74. Girard, A.; Sachidanandam, R.; Hannon, G.J.; Carmell, M.A. A Germline-Specific Class of
692 Small RNAs Binds Mammalian Piwi Proteins. *Nature* 2006, *442*, 199–202,
693 doi:10.1038/nature04917.

694 75. Carmell, M.A.; Girard, A.; Kant, H.J.G. van de; Bourc'his, D.; Bestor, T.H.; Rooij, D.G. de;
695 Hannon, G.J. MIWI2 Is Essential for Spermatogenesis and Repression of Transposons in the
696 Mouse Male Germline. *Dev Cell* 2007, *12*, 503–514, doi:10.1016/j.devcel.2007.03.001.

697 76. Aravin, A.A.; Sachidanandam, R.; Bourc'his, D.; Schaefer, C.; Pezic, D.; Toth, K.F.; Bestor,
698 T.; Hannon, G.J. A PiRNA Pathway Primed by Individual Transposons Is Linked to De Novo
699 DNA Methylation in Mice. *Mol Cell* 2008, *31*, 785–799, doi:10.1016/j.molcel.2008.09.003.

700 77. Brennecke, J.; Aravin, A.A.; Stark, A.; Dus, M.; Kellis, M.; Sachidanandam, R.; Hannon,
701 G.J. Discrete Small RNA-Generating Loci as Master Regulators of Transposon Activity in
702 Drosophila. *Cell* 2007, *128*, 1089–1103, doi:10.1016/j.cell.2007.01.043.

703 78. Gunawardane, L.S.; Saito, K.; Nishida, K.M.; Miyoshi, K.; Kawamura, Y.; Nagami, T.;
704 Siomi, H.; Siomi, M.C. A Slicer-Mediated Mechanism for Repeat-Associated SiRNA 5' End
705 Formation in Drosophila. *Science* 2007, *315*, 1587–1590, doi:10.1126/science.1140494.

706 79. Betel, D.; Sheridan, R.; Marks, D.S.; Sander, C. Computational Analysis of Mouse PiRNA
707 Sequence and Biogenesis. *Plos Comput Biol* 2007, *3*, e222, doi:10.1371/journal.pcbi.0030222.

708 80. Marzec, M. Size Does Matter: PiRNA and MiRNA Targeting. *Trends Biochem Sci* 2021, *47*,
709 287–288, doi:10.1016/j.tibs.2021.12.001.

710 81. Berninger, P.; Jaskiewicz, L.; Khorshid, M.; Zavolan, M. Conserved Generation of Short
711 Products at PiRNA Loci. *Bmc Genomics* 2011, *12*, 46–46, doi:10.1186/1471-2164-12-46.

712 82. Oey, H.M.; Youngson, N.A.; Whitelaw, E. The Characterisation of PiRNA-Related 19mers
713 in the Mouse. *Bmc Genomics* 2011, *12*, 315–315, doi:10.1186/1471-2164-12-315.

714 83. Ichiyanagi, T.; Ichiyanagi, K.; Ogawa, A.; Kuramochi-Miyagawa, S.; Nakano, T.; Chuma,
715 S.; Sasaki, H.; Udono, H. HSP90α Plays an Important Role in PiRNA Biogenesis and
716 Retrotransposon Repression in Mouse. *Nucleic Acids Res* 2014, *42*, 11903–11911,
717 doi:10.1093/nar/gku881.

718 84. Kierszenbaum, A.L.; Tres, L.L. Structural and Transcriptional Features of the Mouse
719 Spermatid Genome. *J Cell Biology* 1975, *65*, 258–270, doi:10.1083/jcb.65.2.258.

720 85. Hecht, N.B. Molecular Mechanisms of Male Germ Cell Differentiation. *Bioessays* 1998, *20*,
721 555–561, doi:10.1002/(sici)1521-1878(199807)20:7<555::aid-bies6>3.0.co;2-j.

722 86. Steger, K. Transcriptional and Translational Regulation of Gene Expression in Haploid
723 Spermatids. *Anat Embryol* 1999, *199*, 471–487, doi:10.1007/s004290050245.

724 87. Fischer, B.E.; Wasbrough, E.; Meadows, L.A.; Randlet, O.; Dorus, S.; Karr, T.L.; Russell, S.
725 Conserved Properties of Drosophila and Human Spermatozoal MRNA Repertoires. *Proc Royal*
726 *Soc B Biological Sci* 2012, *279*, 2636–2644, doi:10.1098/rspb.2012.0153.

727 88. Corral-Vazquez, C.; Salas-Huetos, A.; Blanco, J.; Vidal, F.; Sarrate, Z.; Anton, E. Sperm
728 MicroRNA Pairs: New Perspectives in the Search for Male Fertility Biomarkers. *Fertil Steril*
729 2019, *112*, 831–841, doi:10.1016/j.fertnstert.2019.07.006.

730 89. Sun, J.; Zhao, Y.; He, J.; Zhou, Q.; El-Ashram, S.; Yuan, S.; Chi, S.; Qin, J.; Huang, Z.; Ye,
731 M.; et al. Small RNA Expression Patterns in Seminal Plasma Exosomes Isolated from Semen
732 Containing Spermatozoa with Cytoplasmic Droplets versus Regular Exosomes in Boar Semen.
733 *Theriogenology* 2021, *176*, 233–243, doi:10.1016/j.theriogenology.2021.09.031.

734 90. Alves, M.B.R.; Celeghini, E.C.C.; Belleannée, C. From Sperm Motility to Sperm-Borne
735 MicroRNA Signatures: New Approaches to Predict Male Fertility Potential. *Frontiers Cell Dev*
736 *Biology* 2020, *8*, 791, doi:10.3389/fcell.2020.00791.

737 91. Liu, W.-M.; Pang, R.T.K.; Chiu, P.C.N.; Wong, B.P.C.; Lao, K.; Lee, K.-F.; Yeung, W.S.B.
738 Sperm-Borne MicroRNA-34c Is Required for the First Cleavage Division in Mouse. *Proc*
739 *National Acad Sci* 2012, *109*, 490–494, doi:10.1073/pnas.1110368109.

740
741

742 **FIGURES**

743 **Figure 1.**

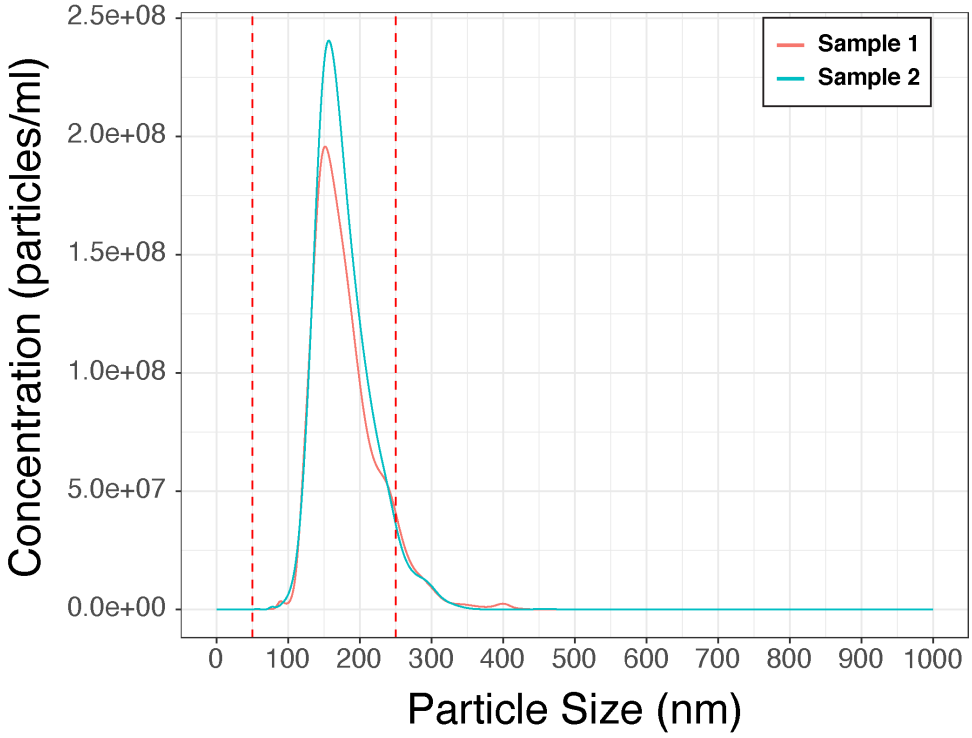

744

745 The size distribution and density of the extracellular vesicles from two separate samples are
746 shown as analyzed by nano-particle tracking (NanoSight 300). The red dashed lines indicate the
747 boundaries of size for canonical epididymosomes (50 – 250 nm [4]).

748

749 **Figure 2.**
750

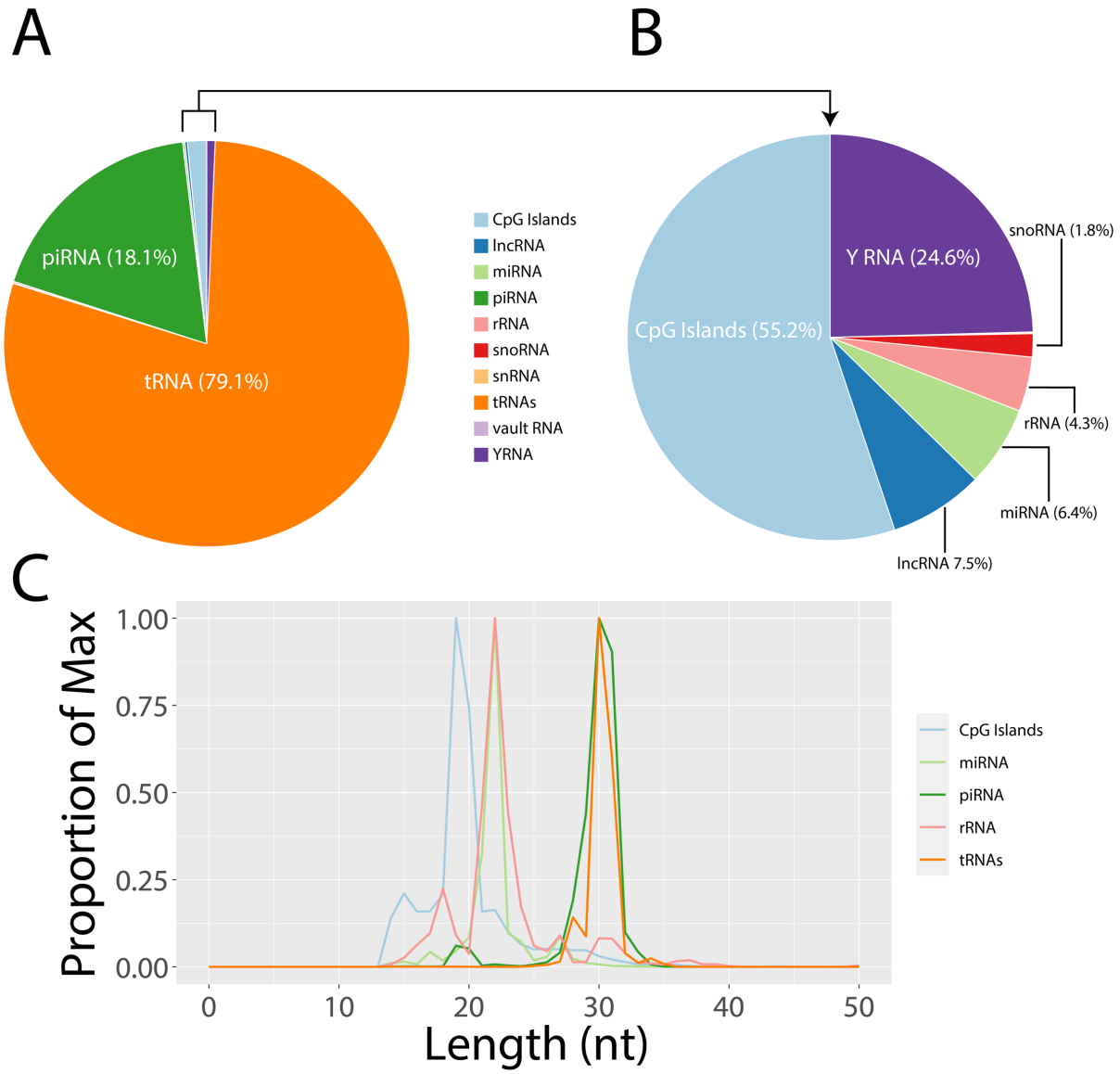

751
752 Results from sequencing small RNA derived from EVs in the rat caput are shown. **A)** The
753 proportion of small RNA reads assigned to each of 10 annotations in our analysis; tRNA and
754 piRNA account for the majority of small RNA in caput EVs while miRNAs are notably absent.
755 **B)** The remaining small RNA reads are shown as a proportion of the residual 2.8% not assigned
756 to tRNA or piRNA loci. CpG islands, which are not a known unit of small RNA expression,
757 account for the majority of the remaining reads. **C)** The size distribution of 4 well-defined
758 sncRNAs are shown and the one undefined category (CpG islands) demonstrates a unique size
759 profile (19 nt). The size distribution for piRNA (29-31 nt) and miRNA (22 nt) are exactly as
760 expected. Reads aligned to tRNA (30 - 31 nt) and rRNA (primary peak at 22 nt and small peaks
761 at 18 nt and 30 nt) both demonstrate size specific fragmentation.

762 **Figure 3.**

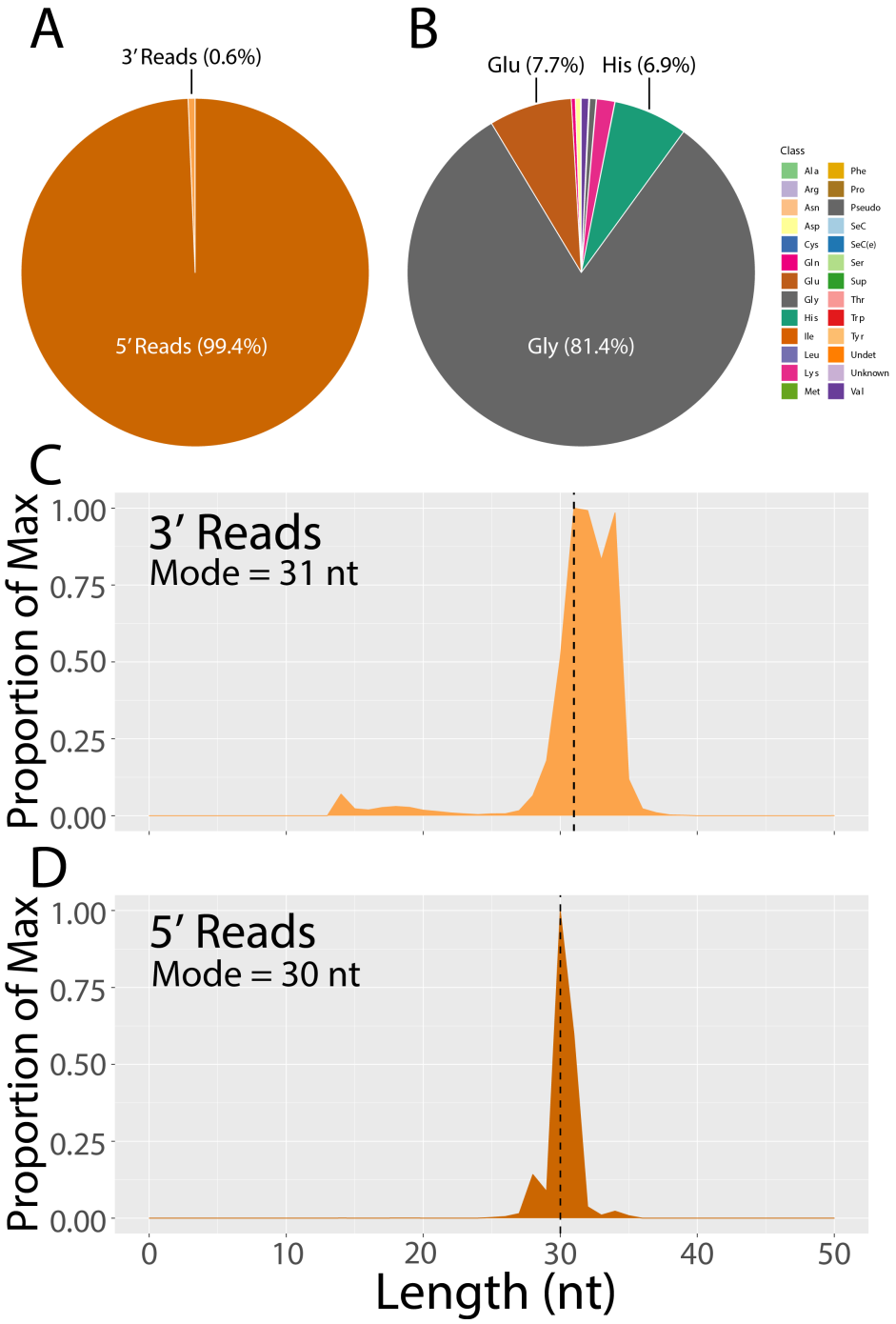

763
764 Detailed analysis of tRNA reads is shown. **A)** Reads align to the 5' end of tRNA loci almost
765 exclusively. **B)** 5'-tRNA^{Gly} is the primary tRNA fragment found in rat caput extracellular
766 vesicles, followed by a substantially smaller proportion of 5'-tRNA^{Glu} and 5'-tRNA^{His}. **C-D)** The
767 size distribution of 3' and 5' tRNA reads are shown, respectively. Reads from the 3' end of
768 tRNA are slightly longer with a broader distribution.

769 **Figure 4.**

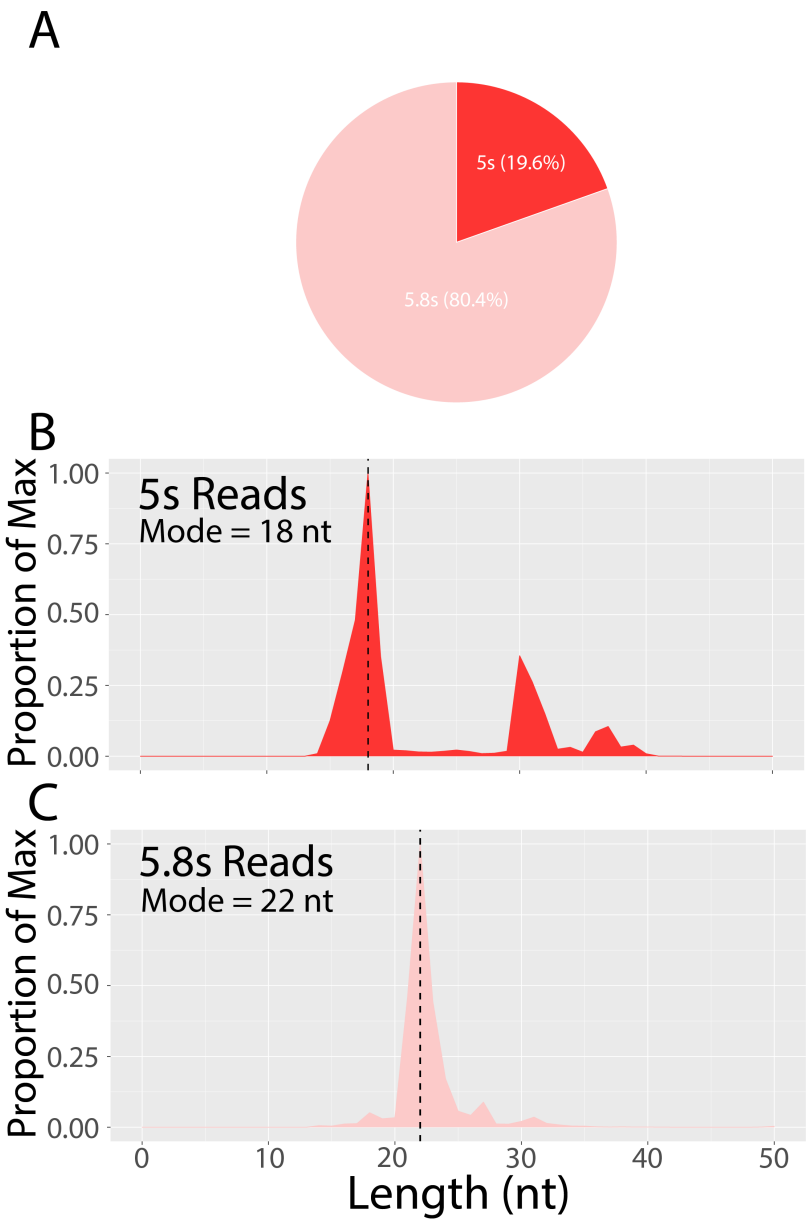

770
771 Reads that aligned to annotated rRNA loci are shown by subcategory. The rat genome is poorly
772 annotated for rRNA, so the available 5s and 5.8s loci were used for categorization. **A)** The
773 majority of rRNA reads aligned to 5.8s rRNA. **B-C)** The size distribution for reads aligned to 5s
774 and 5.8s rRNA show profiles indicative of rRFs that are unique from one another. **B)** 5s rRFs
775 show a bimodal distribution with peaks at 18 and 30 nt. **C)** 5.8s rRFs show a single peak at 22 nt.

776 **Figure 5**

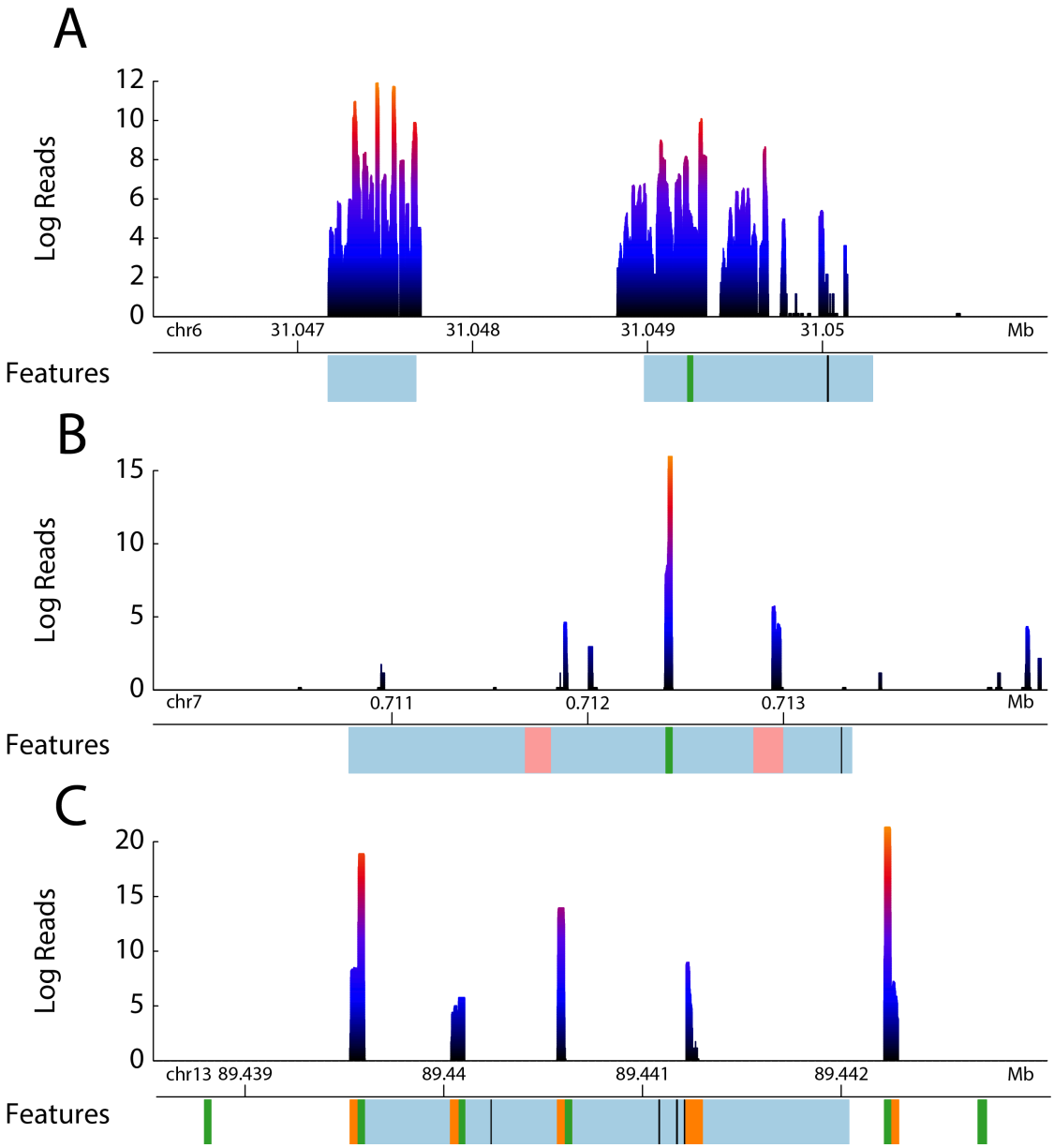

777
778 The log transformed density of reads is shown across three CpG islands with different
779 characteristics. Overlying feature annotations are shown indicated by color; Light blue = CpG
780 island, Green = piRNA, Black = predicted transcriptional start sites, red = 5.8s rRNA, and
781 orange = tRNA. **A)** Reads are shown expressed from within the boundaries of a CpG island on
782 chromosome 6. The reads were not associated with the piRNA (green) within the 3' CpG island
783 while the 5' CpG island had no other overlying features. **B)** Reads were identified within a CpG
784 island on chromosome 7 but the majority of them aligned to a piRNA (green) and rRNA (red)
785 feature. **C)** Reads were identified within a CpG island on chromosome 13 but they aligned
786 exclusively to piRNA and tRNA loci and are demonstrative of their typical expression profiles.
787 The CpG islands from **B & C** (and all other CpG islands like these) were removed from the
788 analysis of small RNAs expressed from CpG islands. The two in **A** are representative of those
789 that were used for further analysis.

Figure 6

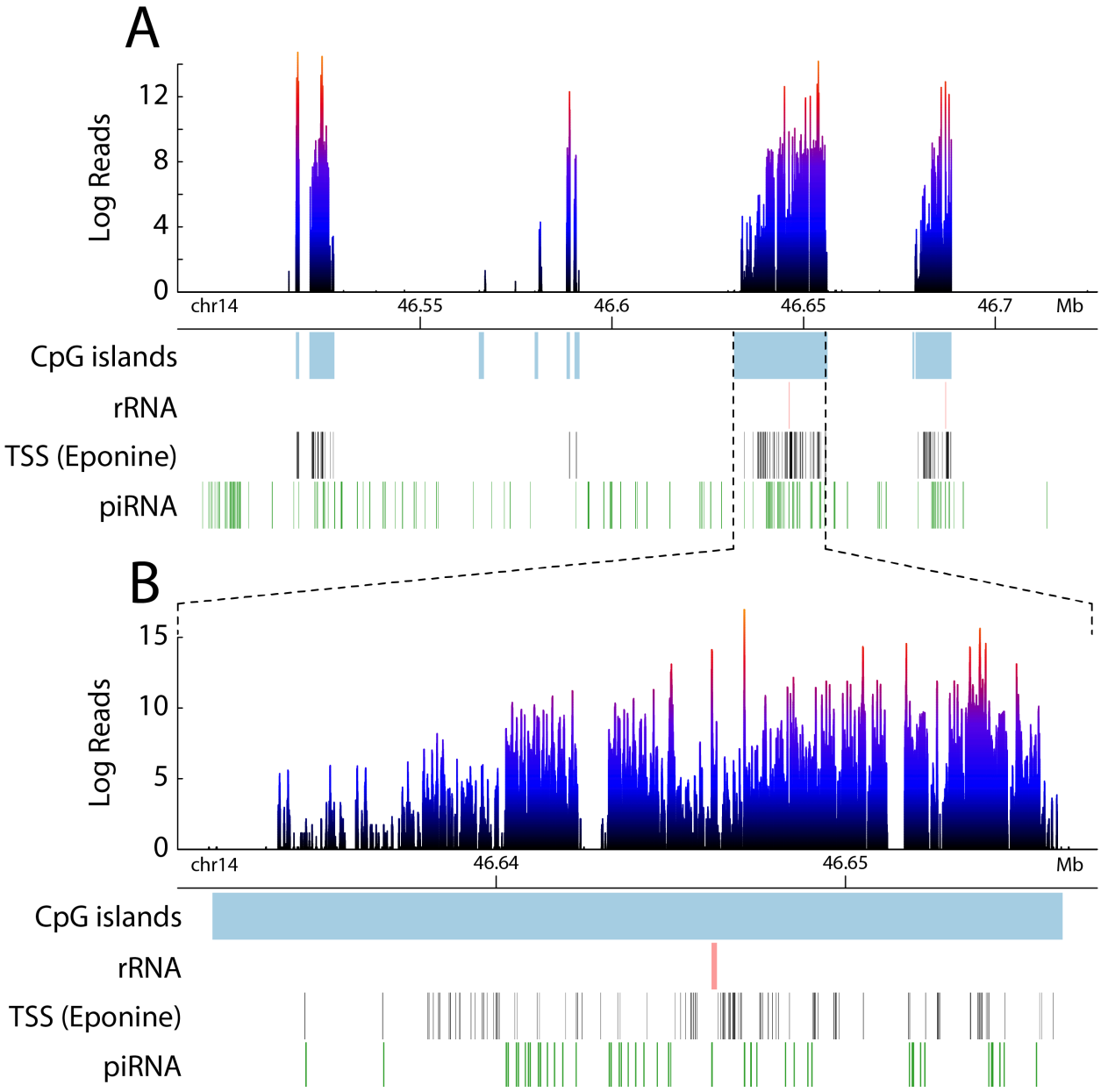

The log transformed reads from a cluster of 8 CpG islands on chromosome 14 are shown with the primary overlying features indicated by color and label. Light blue = CpG islands, Red = 5.8s rRNA, Black = predicted transcriptional start sites, Green = piRNA. **A)** The boundaries of the reads shown are clearly demarcated by CpG islands and not the overlying features such as rRNA or piRNA. **B)** A detailed view of the largest CpG island in the chromosome 14 cluster. The reads are not associated with either the rRNA or piRNA features within the CpG island and are not typical of those features found elsewhere (Figure 5B & C).

TABLES

Table 1

Class	Mode	Median	Mean	SD	90% Range
CpG Islands	19	19	19.89	3.75	15 - 28
lncRNA	22	22	22.27	4.98	15 - 33
miRNA	22	22	22.04	2.34	19 - 27
piRNA	30	30	29.60	2.50	26 - 32
rRNA	22	22	22.65	4.06	17 - 31
snoRNA	27	24	23.44	5.12	15 - 32
snRNA	16	16	18.05	3.85	15 - 26
tRNAs	30	30	30.19	1.18	28 - 31
vault RNA	18	19	22.99	8.02	14 - 41
Y RNA	31	31	28.33	3.89	22 - 31

Descriptive statistics of the read length for each annotated small RNA category are shown with the mode, median, mean, standard deviation, and length range from which 90 percent of the reads are found.

805 **Table 2**

Name	Reads per Million	Found in Sperm	Found in EVs
miR-1b	16.2	--	--
miR-7a-1	19.7	[88]	[89]
miR-7a-2	19.9	[88]	[89]
miR-let-7c	10.0	[88]	[89]
miR-let-7i	11.7	[88]	[89]
miR-26a	11.7	[90]	--
miR-99a	87.8	[91]	--
miR-143	29.5	[19]	[19]
miR-148a	93.0	[88]	[89]
miR-184	493.7	[88]	[89]
AABR07005004.2	16.0		
AABR07029907.2	34.7		
AABR07057421.1	11.9		
AABR07064716.2	34.2		
AABR07064724.1	22.1		

806
807 Fifteen miRNA were identified as having substantial (> 10 RPM) expression in rat caput EVs, 10
808 of which are annotated and 5 that are putative. This is far fewer than expected based on mice
809 experiments. The majority of miRNAs identified have previously been reported in either sperm
810 or EVs (citation indicated), except for miR-1b. A miRNA considered a hallmark of caput EVs
811 (miR-143) was also identified in our rat data set.

812 Table 3.

Chromosome	Start Location	End Location	Length (nt)	Read Count	RPKM	piRNA Loci	pRNA Protein Loci	rRNA Binding Protein Loci	rRNA Loci
Chr 1	11,903,555	11,916,838	13,283	112,070	63.16	19	1	0	1
Chr 1	11,961,297	11,975,108	13,811	278,633	151.02	27	1	0	1
Chr 5	91,124,274	91,141,016	16,742	341,585	152.72	26	1	0	1
Chr 6	30,627,068	30,633,859	6,791	177,949	196.15	13	0	0	2
Chr 6	31,047,175	31,047,676	501	10,347	154.59	0	0	0	0
Chr 6	31,048,983	31,050,286	1,303	3,282	18.85	1	0	0	0
Chr 14	46,517,594	46,518,401	807	113,831	1,055.86	1	0	0	0
Chr 14	46,521,126	46,527,599	6,473	170,612	197.30	10	0	1	0
Chr 14	46,588,206	46,589,034	828	39,955	361.21	0	0	1	0
Chr 14	46,590,294	46,591,521	1,227	2,562	15.63	1	0	1	0
Chr 14	46,631,880	46,656,213	24,333	429,235	132.04	44	0	1	1
Chr 14	46,679,234	46,688,547	9,313	160,403	128.93	17	0	0	1

813

814 The genomic coordinates (Rnor v6 – Chromosome, Start Location, End Location) of 12 CpG
815 islands found to have substantial expression (> 10 RPKM) of ~19nt small RNA transcripts are
816 shown along with the length of the CpG island, raw read count, and length-corrected read count
817 (RPKM) found within each. The number of various overlying features found overlapping each
818 CpG island is also shown.